LES OF FLOW OVER MULTIPLE CUBES

Thorsten Stoesser [1], Fabrice Mathey [2], Jochen Fröhlich [3], Wolfgang Rodi [1]

[1] Institute for Hydromechanics, Karlsruhe University, 76128 Karlsruhe , Germany
[2] Fluent France, 78180 Montigny Le Bretonneux, France
[3] Institute for Chemical Technology, Karlsruhe University, 76128 Karlsruhe, Germany

INTRODUCTION

The flow around multiple cubes mounted on a surface is of practical interest in a variety of areas. One is building aerodynamics where the cubes represent groups of simple, idealized buildings. Here the wind loading caused by the complex flow is of interest and for the urban climate the flow and dispersion in the street canyons. On a larger scale, the effect of groups of buildings as urban canopy roughness elements on the atmospheric boundary layer and its interaction with the urban climate conditions is of concern. Similar mechanisms occur in hydraulics where the bounding walls are usually hydraulically rough and the roughness has a strong influence on the surface flow behaviour, the energy dissipation, the sediment transport and the exchange with the ground water. A great variety of shapes and arrangements of roughness elements exist, but the configuration of a matrix of cubes is ideal for fundamental studies of the processes around the roughness elements and the flow above them. This arrangement is also of special interest in the area of cooling of electronic components where such elements are used to increase greatly the heat transfer compared to that from a smooth wall.

Already the flow around a single surface mounted cube is rather complex with various separation regions and reattachments, horse-shoe vortices wrapping around the cube as well as vortex shedding from the side walls and generally unsteady behaviour dominated by larger flow structures. The flow around multiple cubes is even more complex through the interaction between the various cubes, with a strong influence of the separation of the cubes, their arrangement and the presence of an upper wall if placed in a channel. Because of these complexities and the presence of large unsteady structures, RANS methods have considerable difficulties in predicting such flows and DNS / LES are clearly more suitable methods (Rodi 1997, Hellsten and Rautaheimo 1999). DNS is restricted to low Reynolds numbers so that for solving practical problems LES has to be used. In this contribution, two LES simulations performed by the authors are summarized, one for a matrix of cubes placed in a relatively narrow closed channel (for details see Mathey et al. 1998, 1999) and the other for the situation of cubes as roughness elements in an open channel with depth to cube height ratio of 13 (for details see Stoesser et al., 2003).

NUMERICAL SOLUTION METHOD

The LES code LESOCC developed at the Institute for Hydromechanics (Breuer and Rodi, 1996) was used to perform the simulations. The code solves the filtered Navier-Stokes equations on a curvilinear, block-structured grid discretised with the finite volume method. A non-staggered grid with Cartesian velocity components is used. Both, convective and diffusive fluxes are approximated with central differences of second order accuracy. The SIMPLE algorithm is employed in order to conserve mass and to couple the pressure to the velocity field. Time advancement is achieved by a second order, explicit Runge-Kutta method. LESOCC is highly vectorised and parallisation is accomplished by domain decomposition and explicit message passing via MPI. The subgrid stresses of the filtered Navier Stokes equations are computed using either the Smagorinsky model (Smagorinsky, 1963) or the dynamic approach of Germano et al. (1991).

FLOW SIMULATIONS

Flow at Small Channel Depth (Case 1)

The first simulation concerns the flow around a matrix of surface mounted cubes placed on one of the walls of a 2-dimensional closed channel whose depth h is 3.4 times the cube height H (see Figure1). This case was studied experimentally by Meinders et al. (1997) who placed a matrix of 25 x 10 cubes in the channel and performed measurements around a cube in the 18^{th} row from the inlet where the flow was developed and periodic. The channel Reynolds number is $Re_h = 1.3 \times 10^4$ and the Re_H based on the cube height is 3,823. In the experiment, one cube was heated and the temperature and heat transfer distributions along the cube walls were measured. This flow was a test case for a series of ERCOFTAC/IAHR workshops, the last one held in Helsinki in 1999. The proceedings of this workshop (Hellsten and Rautaheimo, 1999) contain detailed calculation results obtained with two LES methods (including the results presented

below) and one DNS method as well as various RANS methods in comparison with the experiments.

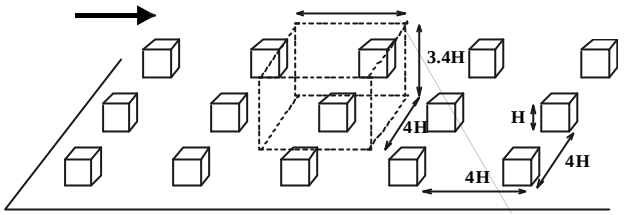

Figure 1: Cube arrangement in the experiment and calculation domain for case 1.

Because of the periodicity and the relatively small channel depth, only the flow around a single cube needed to be calculated, with periodicity conditions employed in the midplanes in the downstream and spanwise directions. The calculation domain having dimensions 4H x 4H x 3.4H is shown in Figure 1. Figures 2, 3 and 4 compare calculated streamlines very near the bottom channel wall, in the vertical symmetry plane, and in a horizontal plane at midheight with the experimental observations. The calculations were carried out on a 100^3 grid using no-slip conditions at all walls. Virtually the same results were obtained with the Smagorinsky and dynamic models and also when switching off the subgrid-scale model. This shows that in this case of fairly low Reynolds number the subgrid-scale model has little influence, which is supported also by the very good agreement with the DNS calculations reported in the workshop proceedings.

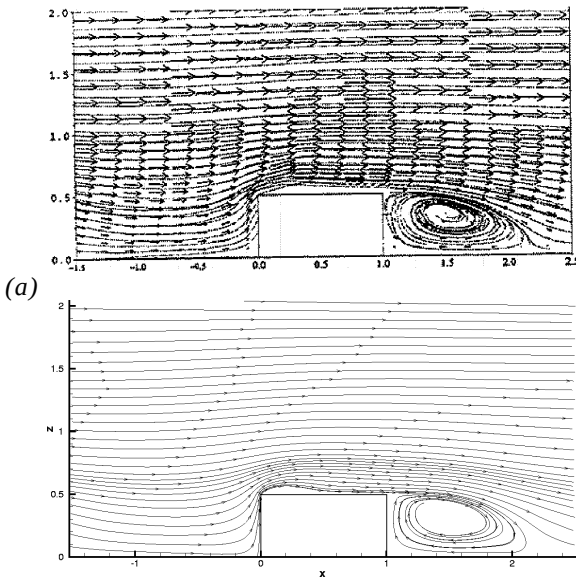

(a)

(b)

Figure 2: Time-averaged streamlines in a horizontal plane at half flow depth for case 1; (a) experiment (b) LES-simulation.

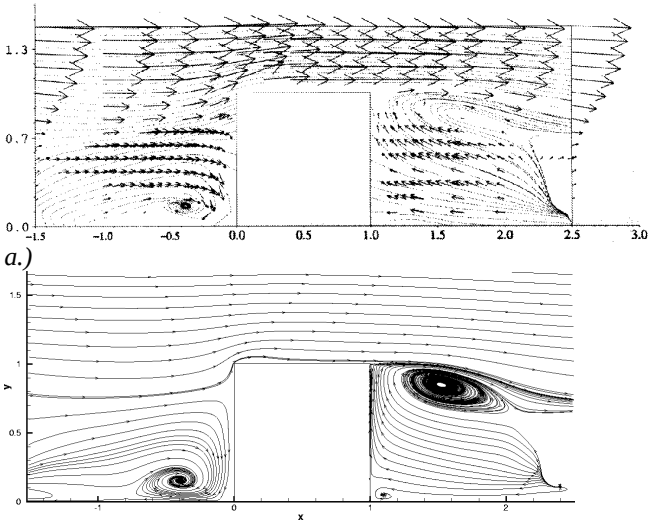

a.)

(b)

Figure 3: Time-averaged streamlines in the vertical symmetry plane for case 1; (a) experiment (b) LES-simulation.

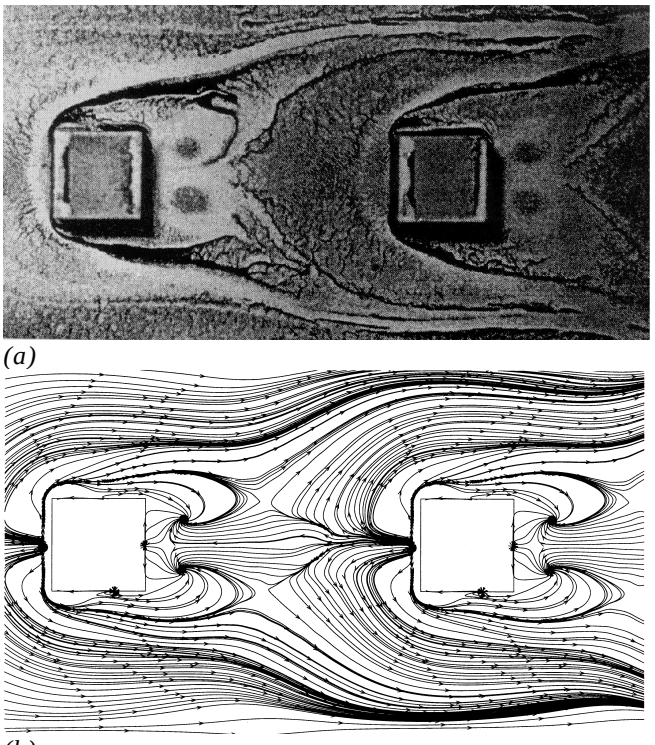

(a)

(b)

Figure 4: Surface streamlines of the time-averaged flow for case 1; (a) oil picture from experiment (b) LES-simulation.

Figures 2 to 4 clearly show the very complex nature of the flow in spite of the simple geometry. The flow separates in front of the cube, the ensuing vortex is bent as a horse-shoe vortex around the cube and is displaced by the horse-shoe vortex formed by the subsequent cube. The flow also separates at the front corners of the cube on the roof and sidewalls but then reattaches so that the

corner separation regions are fairly small. A large separation region develops behind the cube and there is no clear reattachment at the bottom between the two cubes; a rather concentrated vortex forms in the upper part of the separation region and a kind of saddle line in the lower part (Fig. 2). Originating from the groundplate, an arch vortex develops behind the cube (Fig. 4), and in the horizontal mid–height plane is a recirculating separation region behind the cube (Fig. 3). All these complex features of the time-averaged flow are very well reproduced by the LES. Profiles along vertical lines of mean velocity and Reynolds stress components are also in very good agreement with the measurements. As an example the u'u' stress profiles are given in Figure 5 (further profiles can be found in Mathey et al., 1998). In the experiment some vortex shedding from the sides of the cube was observed, and this was also obtained in the LES calculations with the correct frequency (Strouhal number St ˜ 0.11).

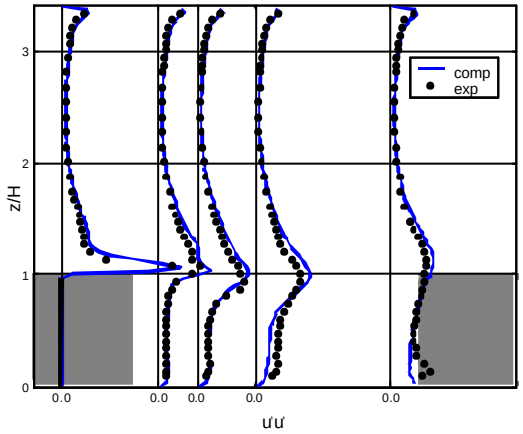

Figure 5: Profiles of u'u' stress in the vertical symmetry plane for case 1.

Figure 6 shows an instantaneous picture of the perturbation velocity vectors i.e. fluctuating velocities subtracted from the mean ones, in the vertical symmetry plane. It illustrates the presence of coherent, vortical motions especially near the cubes. In the vicinity of the cubes, the turbulent stresses are approximately 5 times higher than near the smooth upper wall, showing clearly the effectiveness of the cubes for generating turbulence. Figure 7 exhibits an instantaneous picture of the temperature distribution in the vicinity of the heated cube illustrating how the heat is transported by the turbulent motion. These calculations of heat transfer required a finer grid of 140^3 points. The calculated distribution of wall temperature and heat transfer around the cube is compared in Mathey et al. (1999) with the measurements of Meinders et al. (1997). Generally good agreement was obtained, while the RANS calculations for both the flow and the heat transfer included in the workshop proceedings are on the whole much poorer than the LES calculations.

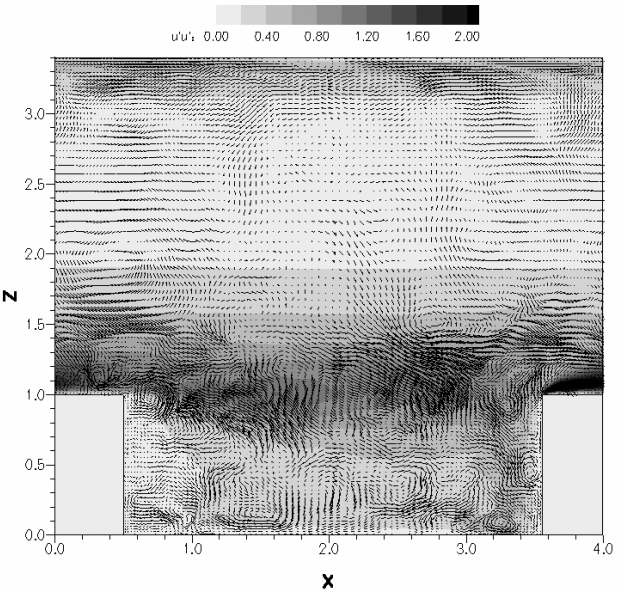

Figure 6: Distribution of u'u' stresses and perturbation velocity vectors in the vertical symmetry plane for case 1.

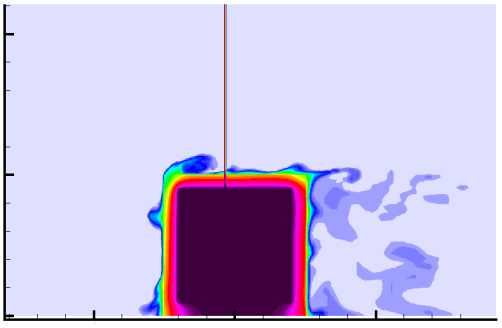

Figure 7: Instantaneous temperature distribution in the vicinity of the heated cube of case 1.

Flow at Large Channel Depth (Case 2)

The second simulation concerns developed flow in an open-channel with a matrix of cubes as roughness elements at the bottom, as studied experimentally by Dittrich et al. (1996). The ratio of channel depth to cube height is 13, the channel Reynolds number is $Re_h = 6 \times 10^4$ and Re_H based on the cube height is 4,192. Figure 8(a) shows a part of the cube matrix in the experiments, where the points a, b, c indicate the locations where vertical profiles of streamwise velocities were measured by LDA. Apart from the much larger h/H ratio, this case differs from the previous case by the fact that the cubes are staggered and closer together. For these reasons, the selection of a computational box around one single element, was inappropriate and the optimum domain size had to be found first through several simulations with different grid resolutions and domain sizes. In this paper we present only the results from the finest grid calculations with 210 x 184 x 156 grid points on the largest domain, of size $15H \times 7.5H \times 13H$ comprising of

32 cubes shown in Figure 8b. It has to be noted that due to the considerably larger domain size relative to the cube dimensions the grid resolution in all three dimensions is much coarser in comparison to the previous case. Substantial grid stretching especially in the vertical direction had to be used. As in case 1, periodic boundary conditions were applied for both the streamwise and spanwise directions. At the lower wall as well as the cube surfaces no-slip conditions were applied with the first grid point placed less than five wall units away from the wall. The upper free surface boundary was approximated with a rigid lid applying symmetry conditions.

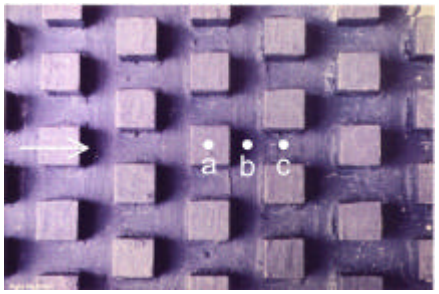

(a)

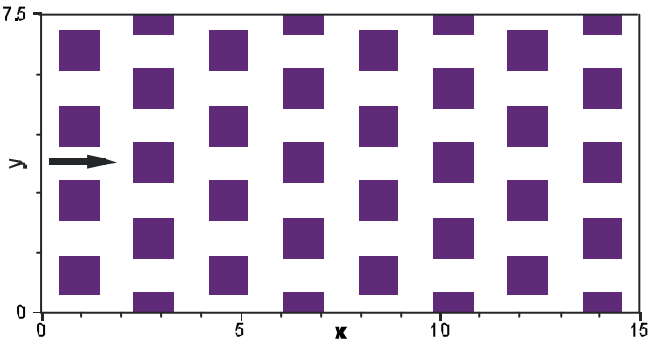

(b)

Figure 8: Cube arrangement and position of measurement verticals for case 2; (a) experiment (b) calculation domain for the LES .

The flow develops several separation and reattachment zones near the roughness elements causing a strong shear layer and a strong disturbance of the flow field in the vicinity of the cubes. This influence prevails up to approximately half of the channel depth. Figure 9 compares the distribution of the mean streamwise velocity with the measurements at the three locations depicted in Figure 8 (a). The agreement is fairly good in Points a and b. However, the recovery of the flow behind the obstacle is underestimated in the simulations as illustrated by the obvious deviation of the streamwise velocity for z/H < 1 at Point c. When comparing the *rms* values of the streamwise velocity fluctuations, at the same locations (Figure 10) it is apparent that along all three measurement verticals a good agreement is achieved. The general feature of rough wall channel flow, i.e. a fairly thick roughness layer and, as a consequence, a relatively large shift of the logarithmic region away from the wall is reproduced. Furthermore, the peaks of streamwise turbulence intensities just above the cubes and the relatively weak gradient observed in the laboratory is predicted.

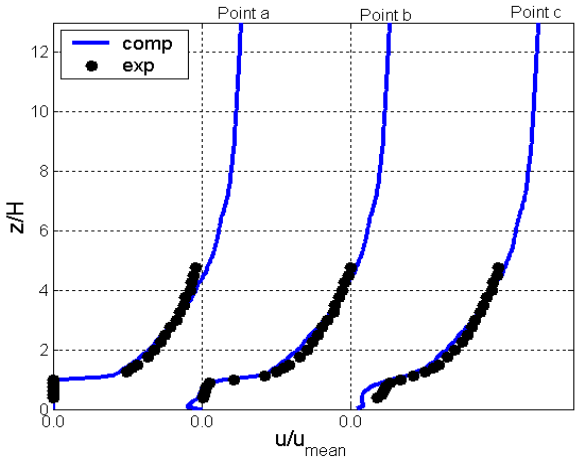

Figure 9: Distribution of time averaged velocities along the 3 measurement verticals for case 2.

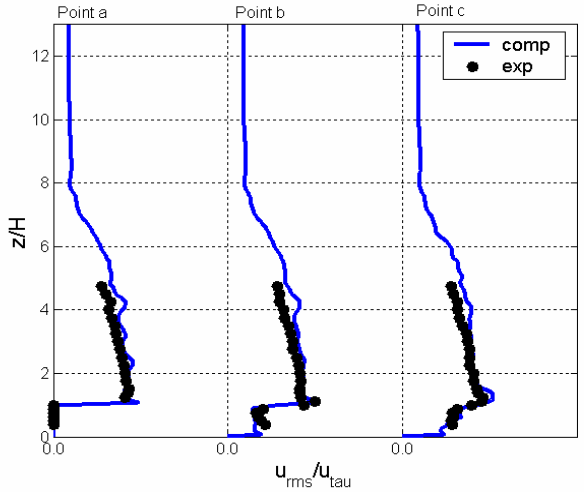

Figure 10: Distribution of u-fluctuations along the 3 measurement verticals for case 2.

Figure 11 shows a snapshot of the instantaneous perturbation velocity vectors in a x-z plane running through the centre of the cubes, while the grey-shading identifies the distribution of streamwise Reynolds stresses. It illustrates the presence of vortical motion, especially near the elements. At position *x » 3* and *z/H » 1*, an ejection event, where slower fluid is ejected towards the free surface, can be detected (see arrow). The rather weak decay of the turbulent motions towards the free surface is also clearly visible.

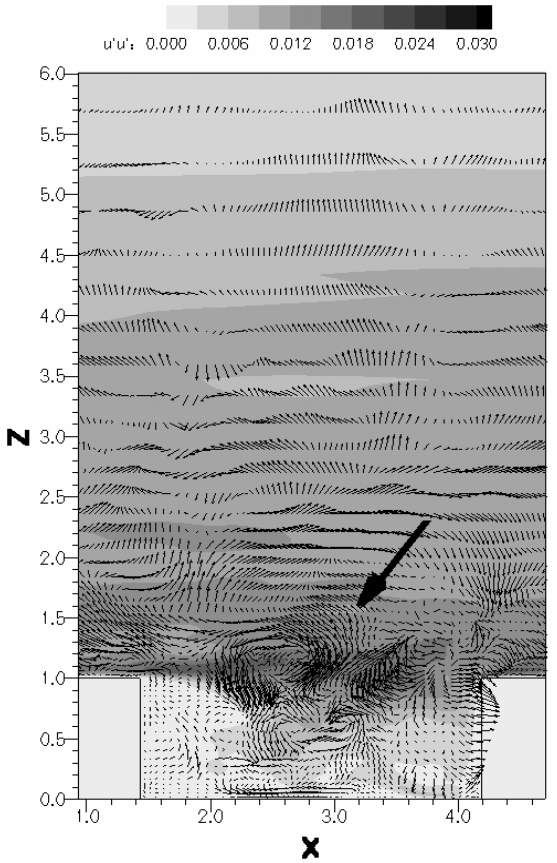

Figure 11: Distribution of u'u' stresses and perturbation velocity vectors in a x-z plane for case 2.

SUMMARY AND CONCLUSIONS

We have presented results of large-eddy simulations of flow over multiple cubes placed in channels of various depths. In the first case considered, the channel depth was relatively small so that the blockage caused by the cubes was fairly large. A very complex flow with various separations and reattachments, horse-shoe vortices and vortex shedding develops around the cubes and influences considerably the entire flow over much of its depth. The second case has a much larger channel depth relative to the cube height and can be regarded as a case with artificially roughened channel bed. A strong form-roughness induced shear layer develops above the elements such that instantaneous and mean velocities differ significantly from those over smooth beds, and the details of the interaction between the flow around the roughness elements and the outer flow could be studied. Overall, the LES simulations showed very satisfactory agreement with the experiments with respect to the mean and fluctuating quantities as well as the development of the complex flow structures. The LES calculations will now be extended to situations with spheres representing the wall roughness and arrays of circular cylinders representing submerged or full-depth obstacles or vegetation which will contribute further to the understanding and predictability of complex flow and turbulence over and around multiple bodies.

ACKNOWLEDGEMENTS

The work reported was funded by the TMR programme of the EU and by the German Research Foundation (DFG). The calculations were carried out on the SNI-VPP300 and SP2 computers of the University of Karlsruhe.

REFERENCES

Breuer, M., Rodi, W. (1996). Large Eddy Simulation of Complex Turbulent Flows of Practical Interest. In: Notes on Numerical Fluid Mech., Flow Simulations with High Performance Computers II. Ed.: Hirschel, E. H. Vieweg, Braunschweig. pp 258-274.

Dittrich A., Nestmann, F., Ergenzinger, P. (1996). Ratio of Lift and Shear Forces Over Rough Surfaces. In: Coherent Flow Structures in Open Channels. Ed.: Ashworth, P. J., et Al. Wiley, New York.

Germano M., Piomelli U., Moin P., Cabot W.H. (1991). A Dynamic Subgrid-Scale Eddy Viscosity Model. Physics Fluids. Vol. 3. pp 1760-1765.

Hellsten, C. J. M., Rautaheimo, P. (Eds.). (1999). Proceedings of the 6th ERCOFTAC/IAHR/COST Workshop on Refined Flow Modelling. June 1999, Rept. 127. Helsinki University of Technology. Helsinki, Finland.

Mathey, M., Fröhlich, J., Rodi, W. (1998). Large Eddy Simulation of the Flow Over a Wall-Mounted Matrix of Cubes. Proc. Workshop on Industrial and Environmental applications of Direct and Large Eddy Simulations. August 5-7th , Istanbul, Turkey.

Mathey, M., Fröhlich, J., Rodi, W. (1999). LES of Heat Transfer in Turbulent Flow Over a Wall-Mounted Matrix of Cubes. In: Direct and Large Eddy Simulation III. Eds.: P. Voke et al.. Kluwer, Dordrecht. pp: 51-62.

Meinders, E. R., Hanjalic, K. (1998). Vortex Structure and Heat Transfer Over a Wall-Mounted Matrix of Cubes. Proceedings of the Turbulent Heat Transfer II Conference, Manchester, June 1998.

Patel, V.C. (1998). Perspective Flow at High Reynolds Number and Over Rough Surfaces - Achilles Heel of CFD. ASME J. Fluids Engineering. Vol. 120. pp 434-444.

Rodi, W. (1997): Comparison of LES and RANS calculations of the flow around bluff bodies, J. Windeng. and Industrial Aerodyn., Vol. 69-71, pp. 55-75.

Smagorinsky, J. S. (1963). General Circulation Experiments With the Primitive Equations, Part 1 Basic Experiments. Mon. Weather Rev. Vol. 91. pp. 99 –164.

Stoesser, T., Fröhlich, J., Rodi, W. (2003). Identification of Coherent Flow Structures in Open-Channel Flow Over Rough Bed Using Large Eddy Simulation. Submitted to the XXX IAHR Conference, Thesaloniki.